

Oxidation of sputtered W-based coatings

A. Cavaleiro^{a,*}, C. Louro^a, F. Montemor^b

^aICEMS-Faculdade de Ciências e Tecnologia da Universidade de Coimbra, Dep. Eng. Mecânica, Polo II, Coimbra, Portugal

^bInstituto Superior Técnico, Lisbon, Portugal

Abstract

In this paper, a review of the influence of the addition of different chemical elements to some transition metal nitrides and carbides on their oxidation behaviour will be presented. The role of the addition of ‘reactive elements’ (RE) on the type of oxide phases formed, on the morphology of the oxide layers, on the oxidation kinetics and on the oxidation rate is emphasized. Examples of the system W–N/C when Ti, Ni and Si are added, will be shown. The beneficial action of the additional element on oxidation resistance can be due either to the formation of some type of protective oxide layer, apart from the typical oxides formed for those metal compounds, or to the blocking effect to the elemental diffusion, which is due to some type of compound precipitation in the diffusion paths. © 2000 Elsevier Science B.V. All rights reserved.

Keywords: Oxidation resistance; W-Based films; Sputtering

1. Introduction

It has been normal procedure in the development of hard coatings to study their behaviour at increasing temperatures in oxidizing environments, after the envisaged value for the mechanical properties has been attained. Several proposals to overcome the mediocre behaviour that some hard coatings show at high temperatures have been presented. Without being exhaustive on this matter, it is of value to refer to some solutions, which have been used to improve the oxidation resistance of these hard coatings:

The addition of ‘reactive elements’ (RE), such as Al, Cr or Si, can act either as preferential nucleation sites in the oxidation process, leading to the formation of a protective scale, or they can form an intermediate oxide layer acting as a diffusion barrier. Moreover, their presence in solid solution, segregated, or as precipitates, can modify the oxide morphology and mi-

crostructure, influencing the diffusion rates and the mechanical properties of the oxide scales.

The deposition of multilayer coatings — the scope is the association of two materials, one of them with a higher oxidation resistance than the other, in order to give the overall coating good oxidation behaviour.

In recent years, the development of alternative metal systems for Ti-based hard coatings has been the aim of our research work. During this development, many transition metal elements (Ni, Fe, Co, Mo, Ti) and others (Au, Si) have been added to the base W–N/C system, in order to improve mechanical properties [1–5]. Similarly to Ti-based systems for some years, the oxidation behaviour also began to be an important factor, due to the poor in-service results achieved by our coatings, in spite of their excellent laboratorial mechanical properties (hardness > 50 GPa, scratch test critical loads higher than 70 N). As a result, the influence of the addition of interstitial (C and N) and other elements (Ni, Ti and Si) on the oxidation behaviour of W films was studied [6–10]. In those studies, besides the comparison of the results of the oxidation resistance, the identification of the mechanisms governing the oxidation of the coatings was one of our main aims.

* Corresponding author. Tel.: +351-239-790-745; fax: +351-239-790-701.

E-mail address: albano.cavaleiro@mail.dem.uc.pt (A. Cavaleiro).

The aim of this paper is to present some typical mechanisms which are known to improve the oxidation resistance of materials, observed on W-based hard coatings deposited by sputtering with different RE when they were subjected to increasing annealing temperatures in air.

2. Experimental procedures

2.1. Deposition technique

The films were deposited by d.c. reactive magnetron sputtering with a specific target power density of 10 W cm^{-2} and a negative substrate bias of 70 V. Targets were W, W–10%Ti and W–10%Ni (mass fractions). In the case of W–Si–N coatings, a W target encrusted with a different number of Si implants was used. When the reactive mode was used, different $(\text{CH}_4/\text{N}_2)/\text{Ar}$ partial pressure was selected, for a total deposition pressure of 3×10^{-3} Pa. The deposition time was selected so that a final thickness in the range of 2–3 μm could be obtained.

2.2. Characterization techniques

Thermogravimetric tests were carried out on a Polymer Science Thermobalance of high-resolution (0.1 μg). Oxidation tests were carried out in industrial air

(99.995% purity) in a temperatures range from 600 to 1000°C. A constant isothermal time of 30 min was generally used.

The structure of the films was analysed by X-ray diffraction (XRD) using a Siemens Diffractometer with $\text{CoK}\alpha$ radiation. A Cameca SX-50 Electron Probe Microanalysis (EPMA) apparatus was used to determine the chemical composition of the coatings. The cross-section of the films (obtained by fracturing the coated samples), its surface topology and morphological details were examined in a Jeol T330 scanning electron microscope (SEM). The Auger analyses were made using a 310 F Microlab (VG Scientific) equipped with a field emission type electron gun, a concentric hemispherical analyser and a differentially pumped ion gun. Auger spectra were taken using a 10 keV, 100 nA primary electron beam. The angle between the primary beam and the surface normal was 30°. The calibration of the analyser was made according to the following peak energies: Cu LMM at 918.62 eV; Ag MNN at 357.80 eV and Au NVV at 70.1 eV.

3. Results and discussion

3.1. Single W coating

The oxidation of single W film is similar to that observed for bulk tungsten. The oxidation law is

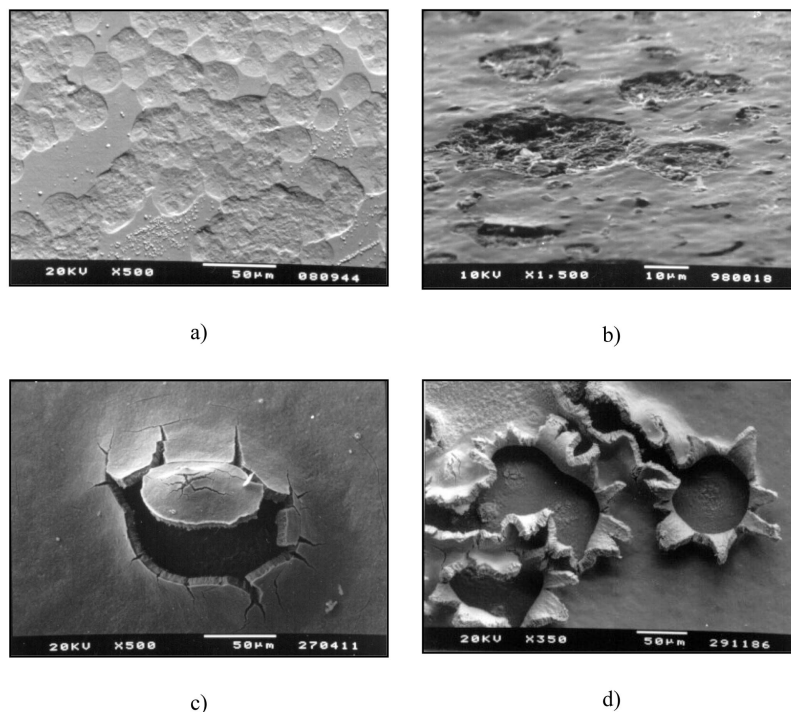


Fig. 1. SEM micrographs showing different types of oxide layers destruction, resulting from the gas evolution during the annealing in air of W–C/N–M sputtered coatings; (a) $\text{W}_{43}\text{Ti}_{13}\text{N}_{44}$, 650°C/60 min; (b) $\text{W}_{24}\text{Si}_{21}\text{N}_{55}$, 850°C/30 min; (c) W_{93}C_7 , 800°C/30 min; (d) $\text{W}_{66}\text{Ni}_{16}\text{N}_{18}$, 750°C/30 min.

parabolic for the range 600–750°C which indicates that the process is controlled by the diffusion of the reactive species (in this case oxygen ions) through the oxide layers. The apparent activation energy ($E_a = 189 \text{ kJ mol}^{-1}$) for the reactions is similar to that presented in the literature for bulk tungsten [7].

The cross-section morphology analysis of the oxidized coatings allows us to distinguish two oxide layers: the inner of which is more compact than the porous outer layer. X-ray diffraction analysis allowed the identification of the inner layer as WO_x and the external as WO_3 [7].

3.2. W + N / C coatings

The addition of interstitial elements C or N to the W sputtered coatings causes, as a general result, a decrease in the weight gain during the oxidation tests, in comparison to a single W film. First of all it should be noted that these elements can not be detected in the oxide layers, i.e. they are lost to the atmospheric environment. Thus, they counterbalance the incorporation of oxygen and the increase in the weight of the sample. On the other hand, in spite of the very low solubility of C/N in the tungsten lattice, it is known that the sputtering technique permits the placing of these elements at high contents in metastable positions in the tungsten. During the oxidation process, at first the oxygen ions substitute C/N in those interstitial positions. These elements can diffuse outwards and/or form molecules of $(\text{CO}, \text{CO}_2)/\text{N}_2$. If the oxidation process proceeds slowly, the molecular gas can diffuse outwards as it is formed. Otherwise, bubbles of these gases can be formed on the interface oxide/coating. The outward diffusion of C/N interferes with the inward oxygen ion flux, which retards their reaction with metal ion on the interface metal/oxide. Moreover, at the outer oxide surface these elements can form a gaseous layer, which lowers the adsorption of molecular oxygen and its dissociation and ionization processes. The limiting step of this reaction should always be the inward diffusion of oxygen ions as is demonstrated by the apparent activation energy of approximately 200 kJ mol^{-1} , very close to that formed for single W film.

When the C/N content in the film (including the W films with Ti, Ni or Si addition) is high enough, the bubbles of molecular gas formed in the interface oxide/coating can reach a significant size, creating stress in the oxide layers which can lead to their destruction. This has several different morphological aspects as shown in the Fig. 1.

This phenomenon is in some cases very severe and it is expressed in the oxidation curves by a sudden abrupt decrease in the weight gain values arising from the loss of flaked oxides from the sample holder in the thermobalance.

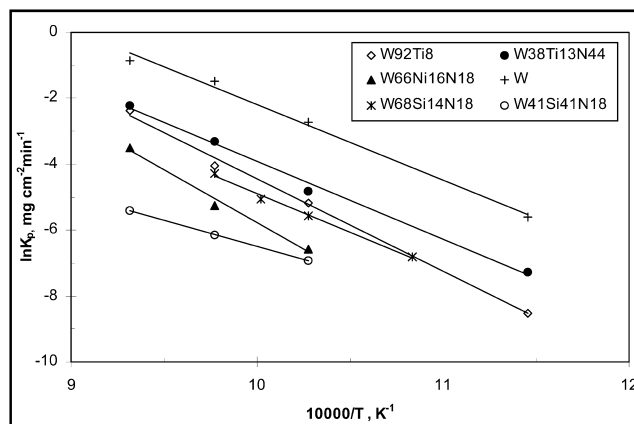


Fig. 2. Arrhenius law for parabolic oxidation of W-C/N-M (M = Ni, Ti and Si) sputtered coatings annealed in air at increasing temperatures.

3.3. W-(N / C) films with M addition

As a general trend, the addition of another element to W-(N/C) sputtered coatings leads to an improvement in their oxidation behaviour. Fig. 2 presents the parabolic rate constants of oxidation as a function of the oxidation temperature for some different types of W-(N/C)-M (M = Ni, Ti and Si) films.

The influence of the addition of M depends on the type of element and also on the presence of N/C in the coating. For example, the W-Ti film has a higher oxidation resistance than the W-Ni film, whereas the inverse is observed between W-Ti-N and W-Ni-N.

The influence of Ti should be different on W-Ti ($E_a = 234 \text{ kcal mol}^{-1}$) and W-Ti-N ($E_a = 197 \text{ kcal mol}^{-1}$) films as is demonstrated in Fig. 2. In fact, the different slope in $\ln K_p = f(1/T)$ curves in this figure suggests different apparent activation energies, and consequently different oxidation mechanisms for both

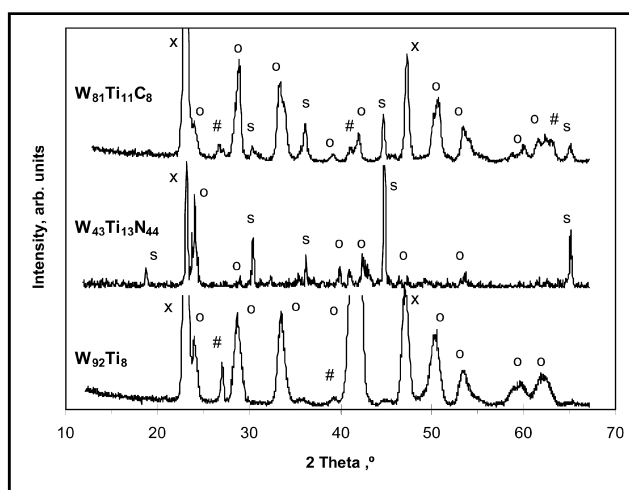


Fig. 3. XRD diffractograms of W-C/N-Ti films oxidized at 800°C; s, substrate; x, WO_x ; o, WO_3 ; #, TiSub2/TiSub30sub5.

coatings. Moreover, the analysis of the X-ray diffractograms obtained at the oxidation temperature, allows us to detect a phase ($\text{TiO}_2/\text{Ti}_3\text{O}_5$) in W–Ti films (Fig. 3) which is not shown in W–Ti–N films. Then, why is there no formation of titanium oxides in the W–Ti–N film, in spite of its higher titanium content in comparison to W–Ti films?

The analysis by EDS of the cross-section of the oxide layers allows us to conclude that there is no agglomeration of titanium oxide in the form of a protective layer, at least with the lateral resolution permitted by the EDS technique. The structure of the as-deposited W–Ti film is the bcc α -W phase, with titanium in solid solution in the tungsten matrix. If the reactivity of Ti for oxygen is compared with that of W ($\Delta H_f^{\text{O-TiO}_2} = -219 \text{ kcal mol}^{-1}$, $\Delta H_f^{\text{O-WO}_3} = -200 \text{ kcal mol}^{-1}$ [11]), it is possible to conclude that titanium can be preferentially oxidized compared with tungsten, but at a very low degree, i.e. tungsten is almost simultaneously oxidized with titanium. Thus, $\text{TiO}_2/\text{Ti}_3\text{O}_5$ oxide must appear in the form of very fine particles (Ti content is much less than W content) in the boundaries of tungsten oxide grains. It is not possible that it can form a continuous layer inside/outside the tungsten oxide layer.

For W–Ti–N film such a situation is not observed. As deposited W–Ti–N has a $\text{W}_2\text{N}/\text{TiN}$ fcc structure. These phases are completely miscible and so titanium (with lower content than W) should be incorporated in the lattice of W_2N . The analysis of W and Ti affinities for oxygen and nitrogen shows that TiN oxidation is less favourable than W_2N ($\Delta H_f^{\text{O-TiN}} = -80 \text{ kcal mol}^{-1}$, $\Delta H_f^{\text{O-W}_2\text{N}} = -17 \text{ kcal mol}^{-1}$ [11]). As happens during the oxidation of metal nitrides there is at first the substitution of N atoms by oxygen ions with nitrogen liberation. The tungsten, which is in higher content in the film, oxidizes first, forming the oxide structure with titanium in substitution of tungsten ions. Thus, the formation of individualized $\text{TiO}_2/\text{Ti}_3\text{O}_5$ grains is avoided.

The action of titanium oxide fine particles should be related to their positioning in the grain boundaries of W oxide grains. In the range of the temperature studied (600–800°C) the diffusion of the reactive species should proceed via grain boundaries [12–14]. If the diffusion is blocked in this way another diffusion mechanism should be activated. This is the case for the W–Ti film. The main oxide phases formed in this film are similar to other W-based films (a double layer of the compact WO_x and the external porous WO_3). Thus, the apparent activation energy (E_a) for the oxidation process, should also be the same. The higher E_a value for W–Ti coatings means that another diffusion mechanism controls the oxidation process. The obstruction of titanium oxide particles to the diffusion via grain boundaries allows that transport by bulk dif-

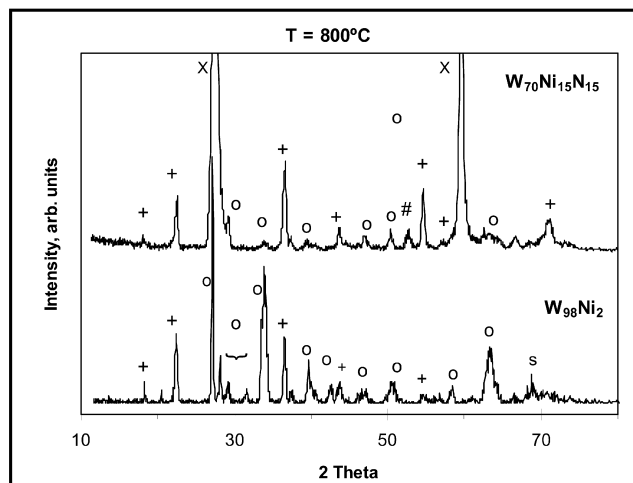


Fig. 4. XRD diffractograms of W–C/N–Ni films oxidized at 800°C; s, substrate; x, WO_x ; o, WO_3 ; +, NiWO_4 ; #, FeWO_4 .

fusion is more feasible, as indicated by the higher apparent activation energy found.

As far as the influence of nickel is concerned, as presented in a previous paper [9], two different mechanisms must be considered to explain the oxidation behaviour of W-based coatings containing nickel, as two different parabolic behaviours can be found on the analysis of the weight gain curves. At low oxidation temperatures and/or short oxidation times an apparent activation energy in the range 180–210 kJ mol^{-1} was calculated, suggesting that the limiting step for oxidation is the inward diffusion of oxygen ions through the WO_x layer. For higher oxidation temperatures an E_a value of 265–295 kJ mol^{-1} was calculated, which suggests another limiting mechanism for the oxidation process. Owing to the higher affinity of W to oxygen in comparison to Ni ($\Delta H_f^{\text{O-NiO}} = -58 \text{ kcal mol}^{-1}$, $\Delta H_f^{\text{O-WO}_3} = -200 \text{ kcal mol}^{-1}$ [11]), W is preferentially

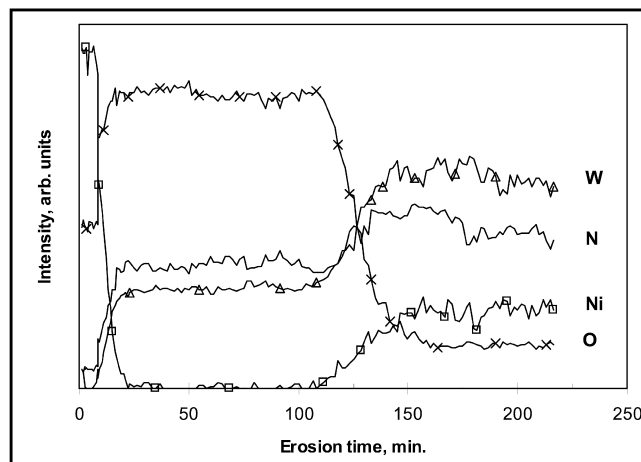


Fig. 5. AES depth profiles of $\text{W}_{70}\text{Ni}_{15}\text{N}_{15}$ coating oxidized at 700°C, 30 min.

oxidized. As this process occurs, the Ni is depleted forming a continuous layer of NiO at the surface. In the interface between NiO and WO_x oxides, W can be combined with NiO forming the $NiWO_4$ spinel. Therefore, for oxidation to proceed it will be necessary for Ni^{2+} ions to diffuse outwards through the WO_x , $NiWO_4$ and NiO layers, to form the NiO oxide on the external surface. However, oxygen will have also to diffuse inward through the WO_x layer. For lower Ni contents (< 5 at.%), the NiO and $NiWO_4$ layers are very thin and the limiting step is the inward diffusion of oxygen ions through the WO_x layer. In this case, both oxidation rates and activation energy similar to those of a single W film were obtained. For higher nickel contents, the limiting step for the oxidation process is the outward Ni^{2+} diffusion through NiO and $NiWO_4$ layers which explains the higher value found for the apparent activation energy. According to some authors [15] these apparent activation energy values are close to those indicated for the oxidation of nickel. For low oxidation temperature/short oxidation time there is no formation of continuous NiO/ $NiWO_4$ layers and the limiting step continues to be the inward diffusion of O^{2-} ions through WO_x layers.

This interpretation was supported by X-ray results that showed the presence of NiO, $NiWO_4$, WO_x and WO_3 phases in the oxidized sample (Fig. 4). EDS on the cross-section of the oxidized sample proved that there was an accumulation of Ni close to the sample surface. Finally, as shown in Fig. 5, it is possible to detect the presence of higher contents of nickel and oxygen and the absence of tungsten near the surface of the oxidized sample, demonstrating the formation of the external NiO layer.

Another point that should be taken into account, during the analysis of the oxidation of these type of coatings, is the structural transformation that they can undergo with temperature increase. When the content

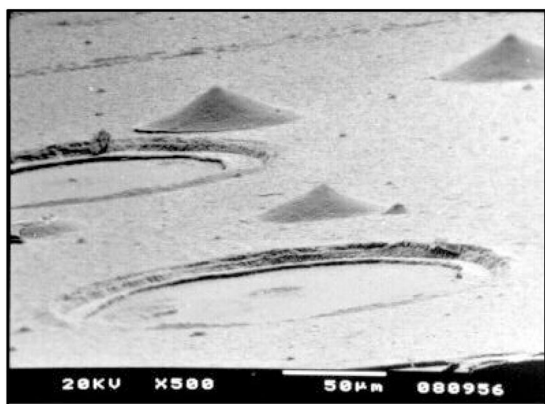


Fig. 6. SEM micrographs showing the preferential oxidation in particular zones of $W_{66}Ni_{18}N_{16}$ sputtered films annealed in air at 750°C, 60 min.

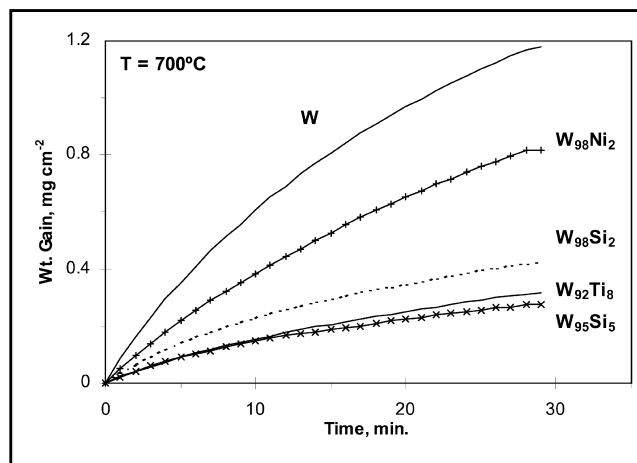


Fig. 7. Isothermal oxidation curves of W-M (M = Ni, Ti and Si) sputtered films annealed in air at 700°C, 30 min.

of nickel is high enough, W-N-Ni coatings have an amorphous as-deposited structure. For temperatures close to 750°C, their crystallization begins to occur in particular zones of the coating. As a result of this transformation important stresses are created that could give rise to the spalling of the protective oxide layers, enhancing coating degradation in those zones (see Fig. 6).

The influence of the addition of silicon on the W-N/C sputtered films is similar to that found for the addition of nickel. For films without nitrogen, the best oxidation resistance is attributed to films containing silicon in comparison to films containing nickel and titanium, if similar contents of these elements are considered (Fig. 7). However, in W-M-N films the inverse is observed (compare in Fig. 8, $W_{68}Si_{14}N_{18}$ and $W_{66}Ni_{16}N_{18}$ films). When higher contents of silicon are considered, better oxidation resistance is obtained in W-Si-N coatings. Moreover, although in Fig. 8 the

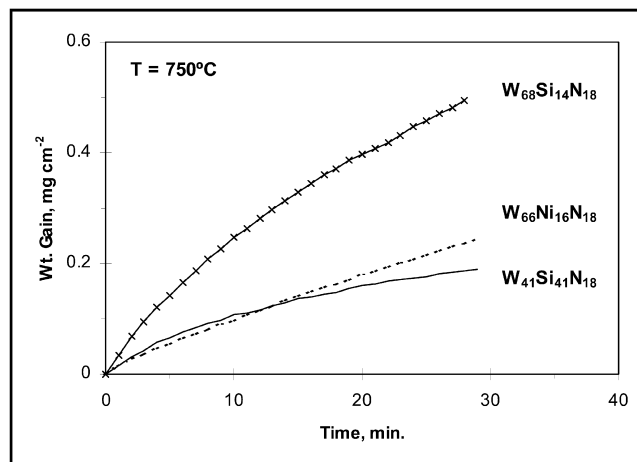


Fig. 8. Isothermal oxidation curves of W-N-M (M = Ni and Si) sputtered films annealed in air at 750°C, 30 min.

isothermal oxidation curves of samples $W_{41}Si_{41}N_{18}$ and $W_{66}Ni_{16}N_{18}$ are very similar, for higher temperatures these differences are enhanced, showing that the $W_{41}Si_{41}N_{18}$ coating has much better oxidation behaviour. It should be noted that the coating containing silicon is only completely oxidized for isothermal annealing at $950^{\circ}C$, whereas $W_{66}Ni_{16}N_{18}$ coating reaches this situation immediately at $800^{\circ}C$.

X-ray diffractograms of the oxidized W–Si–N coatings show approximately the same trends. Fig. 9 presents, as an example, the X-ray diffractogram of samples $W_{41}Si_{41}N_{18}$ and $W_{68}Si_{14}N_{18}$. The oxide peaks are broader than those obtained for W, W–C/N, W–Ti–C/N and W–Ni–C/N coatings and no sign of the so-called WO_x oxide was detected. Moreover, besides the main peak of WO_3 oxide and the peaks belonging to the non-oxidized coating and to the substrate, no other oxide phase, in particular containing silicon, was detected. If the type of the oxides formed during the oxidation process is the same for the coatings containing low and high silicon contents, better oxidation behaviour of high Si films can only be explained by a process similar to that described above for films containing nickel, i.e. only if a certain content in silicon exists in the coating a protective layer can be formed. The existence of this protective layer is clearly demonstrated by using Auger analysis. Fig. 10b shows the results of the AES analysis carried out at consecutive points, following the line shown in the micrograph of Fig. 10a. This picture represents the crater created by the wear induced by a rotating ball on the surface of $W_{69}Si_{31}$ sample. The line shown in the picture goes from the oxide surface, through the oxidized and non-oxidized coating to the substrate. As can be concluded close to the oxide surface only Si and O are detected meaning that a silicon oxide is formed on that zone.

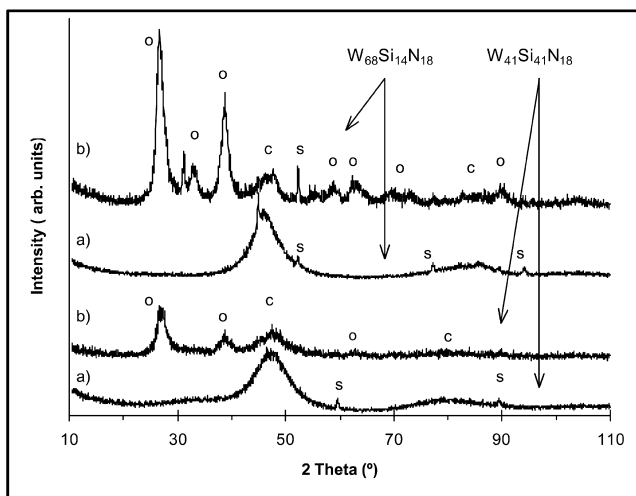
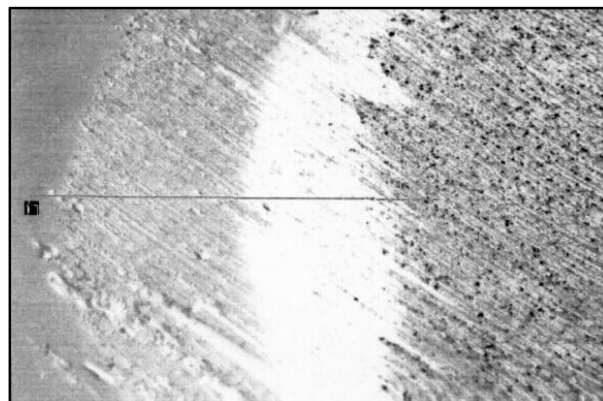
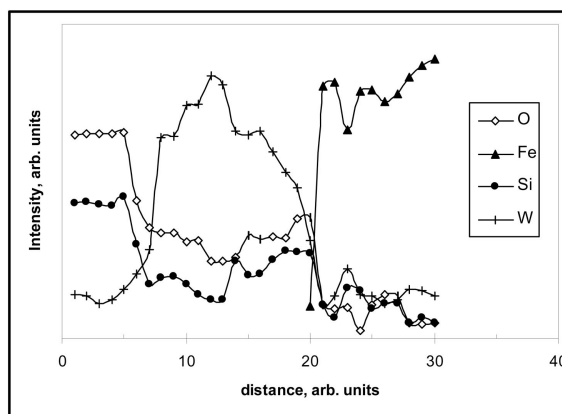


Fig. 9. XRD diffractograms of W–N–Si coatings annealed in air at increasing temperatures; (a) as-deposited; (b) $700^{\circ}C/30$ min.



a)



b)

Fig. 10. AES results obtained from a linear scan performed on the worn zone of the surface of an oxidized $W_{69}Si_{31}$ sputtered coating annealed in air at $850^{\circ}C$, 30 min; (a) SEM micrograph showing the zone of the ball crater when the linear scan was performed (the total line length is 0.6 mm); (b) AES results.

The non-detection of this layer by X-ray diffraction means that it is amorphous. It is well known [16–19] that in the oxidation of Si-based materials a protective amorphous silica layer is built up. The SiO_2 oxide crystallizes only at temperatures higher than $1000^{\circ}C$ [20].

This silicon oxide layer is only efficient in the protection of the coatings against oxidation, if in this case the mechanism that rules oxidation behaviour is ion diffusion through the silicon oxide layer; otherwise, the oxidation rate is controlled by ion diffusion through the tungsten oxide scale. The evaluation of the apparent activation energy for the oxidation of W–Si–N coatings confirms the above mentioned facts. For example, for the above presented $W_{68}Si_{14}N_{18}$ and $W_{41}Si_{41}N_{18}$ coatings the E_a values were 194 kJ mol^{-1} and 130 kJ mol^{-1} , respectively. The first value is similar to that found for the oxidation of tungsten. The other value is

very close to that presented in the literature (120 kJ mol⁻¹) for the diffusion of oxygen in SiO₂ oxide [21].

4. Conclusions

The influence of the addition of different elements to sputtered W-based coatings on their oxidation resistance was studied. Depending on the type of element addition, different mechanisms were identified to understand the oxidation behaviour. The general conclusions for the studied elements were:

1. N and C improves the oxidation resistance of tungsten sputtered coatings, by interfering with inward oxygen diffusion; however, their accumulation in form of bubbles on the interface oxide/coating can lead to flaking of the protective oxide scale;
2. Ti significantly improves the oxidation resistance of the W-sputtered coating, in the case of the formation of TiO₂/Ti₃O₅ oxide as small particles in the grain boundaries of the tungsten oxide layer. These particles obstruct the movement of the oxygen by grain boundaries forcing their inward diffusion by bulk material. This only takes place if the as-deposited structure of the coatings is the α -W phase. For W–Ti–N films with nitride phases W₂N, no independent titanium oxide particles are formed and the improvement is much smaller;
3. Both Ni and Si have a similar significant influence on the oxidation behaviour of W-based coatings. If their content in the as-deposited films is high enough, continuous layers of NiO/NiWO₄ and amorphous Si–O oxides are formed, contributing to a decrease in the ion diffusion rate, which improves oxidation resistance. In some cases, these coatings have as-deposited amorphous structures which after crystallization can induce the flaking of the protective oxide scale, due to dimensional variation. For the film with a high content of silicon, annealing temperatures as high as 950°C can be reached without the total oxidation of the coating during a 30 min isothermal annealing.

Acknowledgements

A travel grant for A. Cavaleiro from Fundação Oriente is acknowledged.

References

- [1] A. Ramalho, A. Cavaleiro, M.T. Vieira, A.S. Miranda, Surf. Coat. Technol. 62 (1993) 536.
- [2] A. Cavaleiro, M.T. Vieira, Surf. Eng. 10 (1994) 147.
- [3] A. Cavaleiro, M.T. Vieira, F. Ramos, J.P. Dias, Thin Solid Films 290/291 (1996) 238.
- [4] C. Louro, A. Cavaleiro, Surf. Coat. Technol. 116–119 (1999) 74.
- [5] B. Trindade, M.T. Vieira, A.M. Amaro, J.S. Cirne, Actas da MRS Spring Meeting, San Francisco, USA, (1998) 1998.
- [6] C. Louro, A. Cavaleiro, Surf. Coat. Technol. 74/75 (1995) 998.
- [7] C. Louro, A. Cavaleiro, J. Electrochem. Soc. 144 (1997) 259.
- [8] C. Louro, A. Cavaleiro, Thin Solid Films 343/344 (1999) 50–55.
- [9] C. Louro, A. Cavaleiro, J. Mater. Process. Technol. 92–93 (1999) 162.
- [10] C. Louro, A. Cavaleiro, Surf. Coat. Technol. 116/119 (1999) 121.
- [11] H.J. Goldschmidt, Interstitial Alloys, Butterworth, London, 1967.
- [12] D.C. Loison, J.C. Pivin, C. Roques-Carnes, Nuclear Instrum. Methods 209/210 (1983) 975.
- [13] M. Pons, M. Caillet, A. Galerir, Nuclear Instrum. Methods 209/210 (1983) 1011.
- [14] R.T. Foley, J.U. Dnuck, R.E. Fryxell, J. Electrochem. Soc. 102 (8) (1955) 440.
- [15] K. Fucki, B. Wagner, Jr, J. Electrochem. Soc. 112 (1965) 384.
- [16] N. Sukifi, C.C. Koch, C.T. Liu, Mater. Sci. Eng. A 191 (1995) 223.
- [17] K.L. Luthra, J. Am. Ceram. Soc. 74 (5) (1991) 1095.
- [18] S. Hampshire, in: D.W. Rens, J.A. Fitzpatrick, D. Taylor, D.M.R. Tapin (Eds.), Proceedings of the 1st Irish Durability and Fracture Conference, Parson's Press, Dublin, 1984, p. 165.
- [19] A.E. Carlsson, P.J. Meschter, in: Westbrook, Fleischer (Eds.), Intermetallic Compounds, 1, Wiley, Sussex, 1994, p. 997.
- [20] D. Bertziss, R.R. Cerchiara, E.A. Gulbransen, F.S. Pettit, G.H. Meier, Mater. Sci. Eng. A 155 (1992) 165.
- [21] P. Hancock, R.C. Hurst, in: R.W. Staehle, M.G. Fontana (Eds.), Advance in Corrosion Science and Technology, Plenum Press, New York, 1974.